# Chapter 9

# FUTURE EXPERIMENTAL FACILITIES

*Conveners:* S. Godfrey, M. A. Sanchis-Lozano

*Authors:* D. Bettoni, P. Crochet, S. Godfrey, F. A. Harris, A. Hoang, O. Iouchtchenko, A. Nairz, J. Napolitano, S. Olsen, P. Petreczki, M. A. Sanchis-Lozano, O. Schneider, A. Zieminski

Opportunities for quarkonium physics abound from a broad range of complementary facilities; CESR-c/CLEO-c, BECP II/BES III, B-factories, CDF and D0 (and BTEV) at the Tevatron, RHIC, GSI, and the LHC. In this chapter we look at these future facilities reviewing and suggesting experimental measurements that can be used as a roadmap for future directions in quarkonium physics.

## 1 TEVATRON

The Tevatron is an existing facility offering an exciting programme on future opportunities for heavy quarkonium physics in the short, medium and long terms (e.g., BTeV, with data taking foreseen in 2009). By August 2004 shutdown, each experiment (CDF and D0) had collected approximately 500 pb$^{-1}$ of data on tape. The number of reconstructed quarkonium states is quite impressive: 2.5 million and 4 million $J/\psi$ candidates collected by D0 and CDF, respectively. D0 reported over 50 000 $\Upsilon(1S)$ events in the data sample corresponding to 200 pb$^{-1}$.

Run II at the Tevatron will provide a substantial increase in luminosity (about 1.4 fb$^{-1}$ delivered to CDF and D0 by the end of 2005 and 8.5 fb$^{-1}$ by 2009) and will allow the collider experiments to determine the $J/\psi$, $\psi(2S)$ and $\chi_c$ cross-sections more precisely and at a larger $p_{\rm T}$ range. An accurate measurement of the $J/\psi$ and $\psi(2S)$ polarization at large transverse momentum will be the most crucial test of NRQCD factorization. In addition, improved data on the $J/\psi$ and $\psi(2S)$ cross-sections will help to reduce some of the ambiguities in extracting the colour-octet matrix elements.

With increased statistics it might be possible to access charmonium states such as the $\eta_c(nS)$ or the $h_c(nP)$. Heavy-quark spin symmetry provides approximate relations between the non-perturbative matrix elements that describe spin-singlet and spin-triplet states. The matrix elements for $\eta_c(nS)$ are related to those for $\psi(nS)$, while the leading matrix elements for $h_c(nP)$ can be obtained from those for $\chi_c(nP)$. Within NRQCD, the rates for $\eta_c(nS)$ and $h_c(nP)$ production can thus be predicted unambiguously in terms of the non-perturbative matrix elements that describe the $J/\psi$, $\psi(2S)$ and $\chi_c$ production cross-sections. A comparison of the various charmonium production rates would therefore provide a stringent test of NRQCD factorization and the heavy-quark spin symmetry. The cross-sections for producing the $\eta_c$ and the $h_c$ at Run II of the Tevatron are large [1, 2], but the acceptances and efficiencies for observing the decay modes on which one can trigger are, in general, small, and detailed experimental studies are needed to quantify the prospects. Other charmonium processes that have been studied in the literature include the production of D-wave states [3], $J/\psi$ production in association with photons [4, 5], and double gluon fragmentation to $J/\psi$ pairs [6].

On the other hand, Run II of the Tevatron will also allow the collider experiments to improve the measurement of the bottomonium cross-sections. As-yet-undiscovered states, such as the $\eta_b(1S)$, could be detected, for example, in the decay $\eta_b \to J/\psi + J/\psi$ [7] or in the decay $\eta_b \to D^* + D^{(*)}$ [8], and the associated production of $\Upsilon$ and electroweak bosons might be accessible [9]. If sufficient statistics can be accumulated, the onset of transverse $\Upsilon(nS)$ polarization may be visible at $p_{\rm T}(\Upsilon) > 15$ GeV.

In sum, the future large statistics data will be used for:

**Production studies**

- Detailed differential cross-section measurements covering the transverse momentum range up to at least 30 GeV and rapidity range up to probably 1.1 (CDF) and 2 (D0), respectively.
- Determination of fractions of quarkonium states produced through the radiative $\chi$ decays. The $\gamma \to ee$ conversions provide a mass resolution sufficient to separate contributions from individual $\chi$ states (both for the $\chi_c$ and $\chi_b$ case). Both experiments have already demonstrated their potential to do such studies.
- Establishment of cross-sections for direct production of quarkonium states ($J/\psi$, $\psi(2S)$, and $\Upsilon(1S)$).
- Measurement of polarization of $J/\psi$, $\psi(2S)$ and $\Upsilon$ states.
- Associated production of quarkonium states, e.g., double $J/\psi$ production.
- Associated production of quarkonium states and heavy quarks, e.g., $J/\psi$ production in association with $c\bar{c}$ pairs.

**Quarkonium decays**

A large sample of $\psi(2S) \to J/\psi\pi^+\pi^-$ decays can be used for a better determination of the dependence of the decay matrix element on the invariant di-pion mass. The observed event accumulation rate is over 5000/fb$^{-1}$ (D0) and 25 000/fb$^{-1}$ (CDF). However, BES accumulated statistics for this channel will be difficult to beat.

**$X(3872)$ state properties**

The two experiments collected approximately 500 (D0) and 750 (CDF) $X(3872) \to J/\psi\pi\pi$ decays per 230 pb$^{-1}$ of data. Studies of the $X(3872)$ properties will continue as the statistics increase. The quantities to measure include the fractions of $X(3872)$ states produced via $b$-quark decays as a function of the production transverse momentum, the decay matrix element dependence on the invariant mass of two final-state pions, $m(\pi\pi)$, and the di-pion resonance contribution to the decay process.

**Searches for exotics decaying into final states involving quarkonia**

CDF searches for strange and charmed pentaquarks have been widely publicized. CDF is also looking for the ($u\ d\ u\ s\ \bar{b}$) pentaquarks decaying into the $J/\psi p$ final state.

**Hadron decays into charmonia**

Exclusive B hadron decays into final states involving a $J/\psi$ have been used for the world's best determination of the $\mathrm{B_s}$ and $\Lambda_b$ masses and their lifetimes. The $\mathrm{B} \to \mathrm{VV}$ decays (where one of the vector decay products is a $J/\psi$) are being used for time-dependent polarization amplitude studies. These studies have led to the determination of lifetime differences of the CP-odd and CP-even $\mathrm{B_s}$ mass eigenstates. They also provide tests of factorization, i.e., representing the weak decay matrix element as a product of two independent hadronic currents.

**$\mathrm{B_c}$ studies**

Both collaborations are advancing their analyses of the $\mathrm{B_c}$ mass and lifetime with Run II data. The yield of observed events in the $\mathrm{B_c} \to \mathrm{J}/\psi\mu + \mathrm{X}$ semileptonic decay channel is approximately 250 events/250 pb$^{-1}$ (D0). These studies require large statistics and a good understanding of the fake muon background in order to reduce systematic uncertainties. A search for exclusive $\mathrm{B_c} \to \mathrm{J}/\psi\pi$ decays is also under way in both experiments.

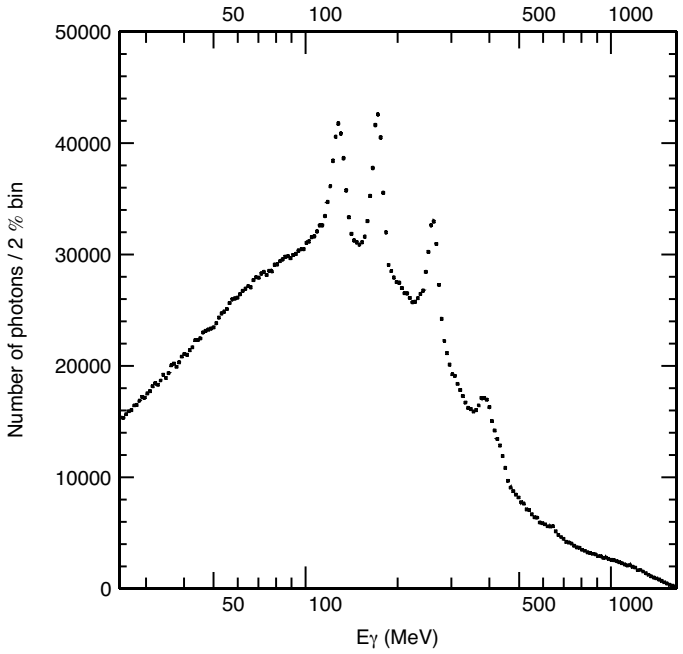


Fig. 9.1: The inclusive photon spectrum from $\psi(2S)$ decay. The data were taken with the CLEO III detector, prior to the CLEO-c upgrade. The peaks from single photon transitions between charmonium states are evident. This already exceeds the data volume acquired by the Crystal Ball at SLAC.

## 2 CLEO-c

CLEO-c is an experiment that makes use of the upgraded CLEO III detector, at the upgraded CESR storage ring. The storage ring (dubbed CESR-c) will use 12 wiggler magnet systems to give increased luminosity at low energies. This section reviews the CLEO-c experimental programme with particular emphasis on charmonium physics. The full details of CLEO-c and CESR-c are available in Ref. [10].

### 2.1 Charmonium physics with the $\psi(2S)$

CLEO-c has already begun taking data on the $\psi(2S)$. The inclusive photon spectrum from the first data set is shown in Fig. 9.1.

More running, with an upgraded CESR and higher instantaneous luminosity, is in the planning stages for the $\psi(2S)$. (In fact, at the time of writing, more data has already been taken.) Depending on running conditions and the will of the collaboration (see Section 2.4), a very large $\psi(2S)$ data set may eventually be accumulated. It is possible that this running may be traded for integrated luminosity on the $J/\psi$ (see Section 2.3).

Potential physics opportunities with the $\psi(2S)$ include the following:

- Inclusive photons. Absolute branching fractions for $\psi(2S)\to\gamma\eta_c$ and $\psi(2S)\to\gamma\eta_c(2S)$ will be measured, although no signal for the former is evident (yet). Note that the mass of the $\eta_c(2S)$ is now accurately known from B-meson decay at Belle [11] and from $\gamma\gamma$ fusion at CLEO [12].
- Detailed studies of $\chi_{c0}$, $\chi_{c1}$, and $\chi_{c2}$. High-statistics single-photon tags of the intermediate $\chi_c$ states will allow various measurements of their decay branching fractions.
- Hadronic decays of $\psi(2S)$. A prime goal is to search for the $h_c$ in $\psi(2S)\to\pi^0 h_c$. The decay $\psi(2S)\to\rho\pi$ will also be searched for, a branching ratio which is anomalously small.
- Exotica from $\psi(2S)$ decay. Radiative decay of high mass vectors is expected to be a prime source for glue-rich final states. (See the discussion in Section 2.3.) Although one expects the majority

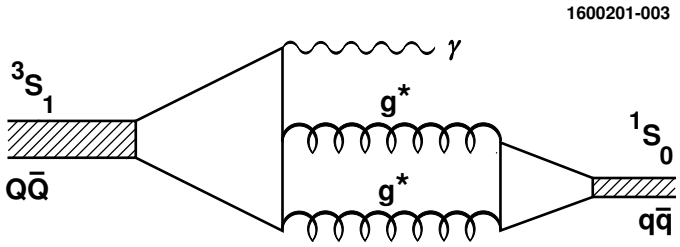


Fig. 9.2: Radiative decay of vector mesons, such as $J/\psi$, to a photon and two gluons. This process is expected to be a copious source of glueballs $X$ via $J/\psi \to \gamma X$.

of this data to come from $J/\psi$ running, $\psi(2S)$ decay would also allow flavour tagging through the hadronic decays where a low-mass vector meson (i.e., $\rho$, $\omega$, $\phi$) replaces the radiative photon. The possibility of studying $J/\psi$ decay using $\psi(2S)$ running and tagging the $J/\psi$ from $\psi(2S) \to \pi\pi J/\psi$ is also being investigated.

### 2.2 Physics at the $\psi(3770)$

CLEO-c has already begun taking a large data sample (eventually 3 fb$^{-1}$) at the $\psi(3770)$. The main goal of this running is to acquire a large sample of tagged D$\bar{\text{D}}$ events, but the opportunity presents itself for charmonium studies as well.

Measurements include searches for (presumably) rare decays of the $\psi(3770)$. Examples are $\psi(3770) \to \pi^+\pi^- J/\psi$; inclusive photons from $\psi(3770) \to \gamma X$, where one would expect to detect transitions to $X = \chi_{cJ}$ if the branching ratio is greater than about $10^{-3}$; and the double cascade decay $\psi(3770) \to \gamma\chi_{c1,c2} \to \gamma\gamma J/\psi \to \gamma\gamma\ell^+\ell^-$ in which one might detect some ten events or so if there is no background and the branching ratio for $\psi(3770) \to \gamma\chi_{c1,c2}$ is more than $\approx 3 \times 10^{-4}$. These results would provide information on $1D_1/2S_1$ mixing.

### 2.3 Decays of the $J/\psi$

An important goal for CLEO-c and CESR-c is to acquire $\approx 10^9$ events at the $J/\psi$ peak. In addition to various rare decay processes, a prime focus will be to study gluonic excitations through radiative decay, i.e., $J/\psi \to \gamma X$. The basic idea is shown in Fig. 9.2. A vector resonance can decay to three (but not two) vector particles. If one of these decay products is a photon, then there is a fair probability that the remaining two are gluons. Hence, this process is expected to give rise to final-state glueballs $X$ [13].

### 2.4 Summary: the CLEO-c schedule

CLEO-c began taking data in October 2003, and has been running smoothly. An upgrade of CESR-c, adding more wigglers for higher luminosity, is on track for spring and summer 2004. The facility will run for approximately three years.

The values of the actual beam energies are decided upon dynamically by the collaboration, and will depend on technical issues as well as emerging physics cases. The original plan [10] is as follows:

- Act I: Obtain 3 fb$^{-1}$ at the $\psi(3770)$, yielding $\sim 1.5 \times 10^6$ D$\bar{\text{D}}$ events.
- Act II: Obtain 3 fb$^{-1}$ at $\sqrt{s} \approx 4.1$ GeV, yielding $\sim 3 \times 10^5$ tagged $\text{D}_\text{s}$ decays.
- Act III: Obtain $10^9$ $J/\psi$.

CLEO-c was encouraged by the QWG to consider running at the $\psi(2S)$ for a long period of time, making use of $\psi(2S) \to \pi\pi J/\psi$ to tag $J/\psi$. This prospect is being studied, including determination of the final-state polarization of the $J/\psi$ and detector acceptance issues, as they relate to the ability to carry out a partial wave analysis.

Table 9.1: Main parameters of BEPCII in comparison with BEPC

| **Parameters** | **Unit** | **BEPCII** | **BEPC** |
|---|---|---|---|
| Operation energy ($E$) | GeV | 1.0–2.1 | 1.0–2.5 |
| Injection energy ($E_{inj}$) | GeV | Up to 1.89 | 1.3 |
| Circumference ($C$) | m | 237.5 | 240.4 |
| Revolution frequency ($f_r$) | MHz | 1.262 | 1.247 |
| Lattice type | | FODO + micro-$\beta$ | FODO + low–$\beta$ |
| $\beta^*$–function at IP ($\beta_x^*/\beta_y^*$) | cm | 100/1.5 | 120/5 |
| Natural energy spread ($\sigma_e$) | | 2. 73E$\times 10^{-4}$ | 2.64E$\times 10^{-4}$ |
| Damping time ($\tau_x/\tau_y/\tau_e$) | | 25/25/12.5 at 1.89 GeV | 28/28/14 at 1.89 GeV |
| RF frequency ($f_{rf}$) | MHz | 499.8 | 199.533 |
| Harmonic number ($h$) | | 396 | 160 |
| RF voltage per ring ($V_{rf}$) | MV | 1.5 | 0.6–1.6 |
| Bunch number ($N_b$) | | 93 | 2$\times$1 |
| Bunch spacing | m | 2.4 | 240.4 |
| Bunch current ($I_b$) | mA | 9.8 at 1.89 GeV | 35 at 1.89 GeV |
| Beam current (colliding) | mA | 910 at 1.89 GeV | 2$\times$35 at 1.89 GeV |
| Bunch length ($\sigma_l$) | cm | $\sim$1.5 | $\sim$5 |
| Impedance ($\lvert Z/n\rvert_0$) | $\Omega$ | $\sim$0.2 | $\sim$4 |
| Crossing angle | mrad | $\pm$11 | 0 |
| Vert. beam–beam param. ($\xi_y$) | | 0.04 | 0.04 |
| Beam lifetime | hrs | $\sim$2.7 | 6–8 |
| Luminosity at 1.89 GeV | $10^{31}$ cm$^{-2}$s$^{-1}$ | 100 | 1 |

## 3 THE BEPCII/BES III PROJECT

The Beijing Electron–Positron Collider (BEPC) is going to have a major upgrade, called the BEPCII project. The BEPCII feasibility report has been officially approved by the Chinese government.

The main physics goals of BEPCII are precision measurements and searches for new particles and new phenomena, mainly in the energy region from the $J/\psi$ to the $\psi(3770)$. For example, precision measurements of D and $\mathrm{D_s}$ meson decays will be essential to allow the CKM matrix parameters, $V_{cs}$ and $V_{cd}$, to be determined with a precision of a few per cent. Studies of light hadron spectroscopy and glueball candidates with very high statistics will be necessary to test QCD, in particular lattice QCD calculations, which should reach precisions of a few per cent in the coming years. Searches for $\mathrm{D^0\bar{D}^0}$ mixing are important to look for physics beyond the Standard Model. The number of important physics topics in the $\tau$-charm energy region is very large.

Our physics goals require major upgrades of the BEPC to increase its luminosity by two orders of magnitude and the BES detector to reduce its systematic errors, as well as to adapt to the small bunch spacing and high event rates. The large-scale upgrade will enable BEPC to approach the specifications of a factory-type machine, whose main parameters are listed in Table 9.1, along with a comparison to those of the current BEPC.

BEPCII will be a double-ring collider with superconducting micro-$\beta$ magnets, a 500 MHz RF system with superconducting cavities, and a low-impedance antechamber beam pipe. The second ring can be accommodated in the existing BEPC tunnel. BEPCII will have a large horizontal crossing angle of 11 mrad at the southern interaction region. There will be 93 bunches per ring with a total current of 910 mA in each ring. The peak luminosity of BEPCII will be $10^{33}$cm$^{-2}$ s$^{-1}$ at the beam energy of 1.89 GeV, which is about 100 times higher than that of the BEPC. The peak luminosity at the $J/\psi$ and at

4.1 GeV c.m. energy will be about $0.6 \times 10^{33}\text{cm}^{-2}\ \text{s}^{-1}$. The upgrade of the linac will provide full energy injection up to 1.89 GeV for 'topping off' the beam. The positron injection rate will reach 50 mA/min compared to the present rate of about 5 mA/min. The number of events expected for one year of running for various physics topics is given in Table 9.2.

Table 9.2: Number of events expected in one year of running

| Physics channel | CM energy (GeV) | Peak luminosity ($10^{33}\text{cm}^{-2}\text{s}^{-1}$) | Physics cross-section (nb) | Number of events per year |
|---|---|---|---|---|
| $J/\psi$ | 3.097 | 0.6 | $\sim$3400 | $10 \times 10^9$ |
| $\tau$ | 3.67 | 1.0 | $\sim$2.4 | $12 \times 10^6$ |
| $\psi(2S)$ | 3.686 | 1.0 | $\sim$640 | $3.0 \times 10^9$ |
| $D$ | 3.770 | 1.0 | $\sim$5 | $25 \times 10^6$ |
| $D_s$ | 4.030 | 0.6 | $\sim$0.32 | $1.0 \times 10^6$ |
| $D_s$ | 4.140 | 0.6 | $\sim$0.67 | $2.0 \times 10^6$ |

Most of the existing utility facilities of the BEPC, after some upgrading, will be used for BEPCII. A cryogenics system of 1000 W at 4.2 K will be installed for the three different superconducting devices. The design of BEPCII will keep the electron beam in the outer ring during the dedicated synchrotron radiation running, and all synchrotron radiation beam lines and the experimental stations will be unchanged, but the beam current will be increased from 140 mA at 2.2 GeV to 250 mA at 2.5 GeV.

BEPCII is a high luminosity, multi-bunch collider, which requires a comparable high quality detector with modern technology. The main features of the detector are as follows (a schematic view of the BES III detector is shown in Fig. 9.3):

- Main draft chamber (MDC): the design features small cell structure, aluminium filled wires, and He-based gas, with expected performances of $\sigma_{xy}$ = 130 $\mu$m, $\Delta p/p$ = 0.5% at 1 GeV, and $dE/dx$ = 6–7%. The stepped end plates provide space for the superconducting micro-$\beta$ magnets;
- Electromagnetic calorimeter (EMCAL): CsI crystals of 15 radiation length (28 cm), with expected performances of $\Delta E/E$ = 2.5 % at 1 GeV and $\sigma_{pos}$ = 0.5 cm/$\sqrt{E}$;
- TOF: plastic scintillators with $\Delta T$ = 90 ps for the barrel part and $\Delta T$ = 100 ps for the end caps;
- 1 tesla superconducting solenoidal magnet;
- Resistive Plate Chambers (RPC) for muon identification: nine layers interleaved with the iron plates of the return yoke;
- Trigger: largely based on FPGA technology and using information of the MDC tracks and EMCAL showers, pipelined with a time latency of 6.4 $\mu$s.

The total estimated budget for the BEPCII will be around 640 million Chinese Yuan (about $77 million). The Chinese government will provide funding to cover the costs of the machine and the major part of the detector. Part of the detector cost is expected to be provided by international contributions. International cooperation is already helping IHEP with the design and R&D of BEPCII, as well as the production of some key devices, e.g., Brookhaven National laboratory is helping with the superconducting micro-$\beta$ magnets; KEK is helping with the superconducting RF cavities and the superconducting solenoid magnet.

The preliminary design of BEPCII has been finished. The engineering design is under way and most parts are finalized. Contracts are already signed for many important items. The project is expected to be completed by the end of 2006, and physics running is scheduled in 2007.

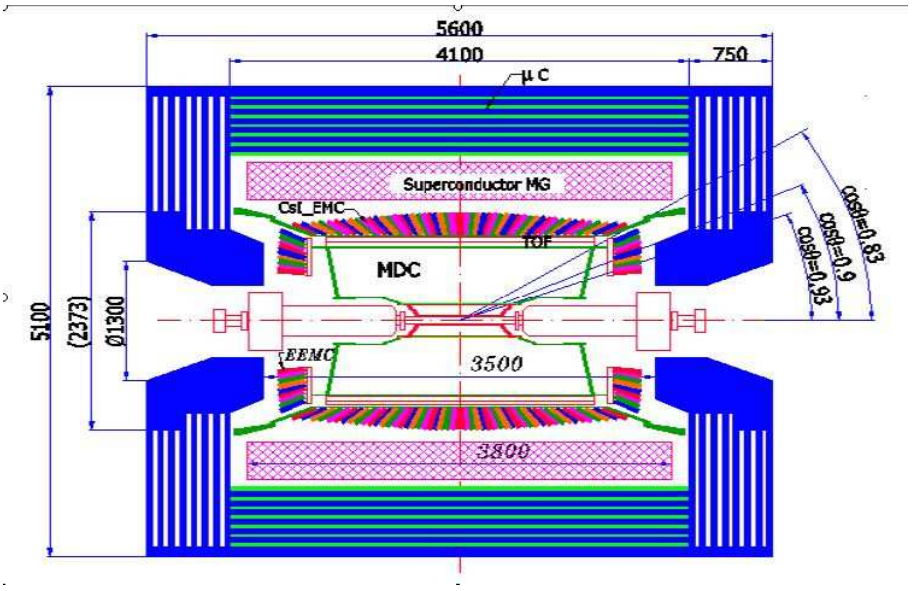


Fig. 9.3: Schematic view of the BES III detector

The great physics potential of BEPCII/BES III will attract the interest of many physicists who are warmly welcomed to join the BEPC/BES upgrade and its physics programme. The completion of the BEPC II will add a new machine of 'factory class' to the fabric of high-energy physics, thus adding new momentum to the research efforts in $\tau$-charm physics.

## 4 B-FACTORIES

One of the goals of a Super B-factory is the search for new physics in B-meson decays. In addition, a very interesting programme on quarkonium physics can be undertaken since $b$ decays are good sources of $c\bar{c}$ states. In this section we shall focus on the KEKB facility, although similar expectations and physical potential apply equally to the SLAC PEPIII project. In particular, there is a proposal to upgrade KEKB to a Super KEKB with a design luminosity of $5 \times 10^{35}$ cm$^{-2}$s$^{-1}$ which is 50 times the peak luminosity achieved by KEKB. The target annual integrated luminosity is 5 ab$^{-1}$.

Along with the luminosity upgrade the Belle detector would be upgraded. The largest challenge will be the very harsh background environment due to the high beam current. Another challenge is the background level in the end-cap and an upgrade to another advanced technology is necessary. Among the candidates, pure CsI crystals with photo tetrode readout is the most promising for the end-cap electromagnetic calorimeter (EECL) and tiles of plastic scintillator with silicon photomultipliers (SiPM) is a good candidate for the end-cap $K_L^0$ muon system (EKLM). The trigger and data acquisition systems should be upgraded to handle the 20 times higher occupancy level from the higher beam current. Computing is another technological challenge with online data having to be recorded at a speed of 250 MB/s after online reconstruction and reduction amounting to the data size of 5 PB/year. Including Monte Carlo simulations, a storage system holding 10–20 PB is needed at the beginning which should be expandable to several tens of PB.

In B-meson decays the $b \to c\bar{c}s$ subprocess is CKM-favoured so that final states containing charmonium particles are common. A super-B factory would provide superb opportunities for high-sensitivity measurements of the charmonium system and the discovery of missing charmonium states such as the $h_c$, or the D-wave states:

– in the continuum: $e^+e^- \to \chi_{c1}\ (c\bar{c})$; $\eta_c\ (c\bar{c})$; search for $C = -1$ states ($h_c$, etc.) in the $\chi_{c1}$, $\eta_c$ recoil spectra;

– in B decays, either with exclusive channels like $B \to K\ 1^3D_2$ (how big is the suppression factor?) or with inclusive channels like $B \to 1^3D_2 \to \pi^+\pi^- J/\psi$ at the $\Upsilon(4S)$.

Another exciting possibility is the discovery of one or more charmonium hybrid states. B-factories can also shed light on the possibility of $D\bar{D}$ molecules. The discovery of the $X(3872)$ just above $D^0\bar{D}^{*0}$ threshold by the Belle Collaboration has led to speculation that the $X(3872)$ is a $D\bar{D}^*$ molecule or some other 4-quark object. The high statistics available at a super B-factory would allow detailed studies of the $X(3872)$ and other new states, including $D\bar{D}$ molecules if they exist.

## 5 GSI

### 5.1 Introduction

The charmonium spectroscopy physics programme of the PANDA ($\overline{P}$ ANnihilations at DArmstadt) experiment using $\overline{p}p$ annihilations at GSI [14] is an extension of successful experiments performed recently at the Fermilab antiproton accumulator. Advanced $\overline{p}$ cooling techniques and a more versatile detector setup will be employed, allowing for the first time the measurement of both electromagnetic and hadronic decays. The goal is to make comprehensive measurements of the spectroscopy of the charmonium system and hence provide a detailed experimental study of the QCD confining forces in the charm region to complement theoretical investigation.

Unlike $e^+e^-$, where only states with the quantum numbers of the photon ($J^{PC} = 1^{--}$) can be formed directly, all quantum numbers are directly accessible in $\overline{p}p$ annihilation. Charmonium states are studied by accelerating the $\overline{p}$ beam to the energy of the resonance, which is then scanned by changing the beam momentum in small steps.

The experimental programme of PANDA also includes the study of gluonic excitations (glueballs and hybrids) in the charmonium sector, as well as the study of charmonium in nuclei.

### 5.2 Experimental apparatus

The PANDA experiment will be installed at the High Energy Storage Ring (HESR), a major component of the recently approved new accelerator facility at GSI in Darmstadt, Germany [14]. The antiproton beam will be produced by a primary proton beam from the planned fast cycling, superconducting 100 T·m synchrotron ring. The antiprotons will be produced with a rate of approximately $2 \times 10^7$/s and then stochastically cooled; after $5 \times 10^{10}$ $\overline{p}$ have been stored, they will be transferred to the HESR where internal experiments in the momentum range from 1 to 15 GeV can be performed. Two modes of operation are foreseen: a high-luminosity mode, where peak luminosities of $2 \times 10^{32}$ cm$^{-2}$s$^{-1}$ will be reached with a beam momentum spread $\delta p/p \approx 10^{-4}$, achieved by means of stochastic cooling in the HESR ring, and a high-resolution mode, where for beam momenta below 8 GeV electron cooling will yield a smaller beam momentum spread $\delta p/p \approx 10^{-5}$ at a reduced luminosity of $10^{31}$cm$^{-2}$s$^{-1}$.

The proposed PANDA detector is being designed to study the structure of hadrons in the charmonium mass range as well as the spectroscopy of double hypernuclei. The detector must provide (nearly) full solid-angle coverage, it must be able to handle high rates ($2 \times 10^7$ annihilations/s) with good particle identification and momentum resolution for $\gamma$, e, $\mu$, $\pi$, K and p. Additional requirements include vertex reconstruction capability and, for charmonium, a pointlike interaction region, efficient lepton identification, and excellent calorimetry (both resolution and sensitivity to low-energy photons).

A schematic view of the present detector concept is shown in Fig. 9.4. The antiprotons circulating in the HESR hit an internal hydrogen pellet (or jet) target, while for the nuclear target part of the experimental programme wire or fibre targets will be used. The detector consists of a Target Spectrometer (TS) and a Forward Spectrometer (FS).

The TS, for the measurement of particles emitted at laboratory polar angles larger than 5°, is located inside a solenoidal magnet, 2.5 m in length and 0.8 m in inner radius. Its main components are four

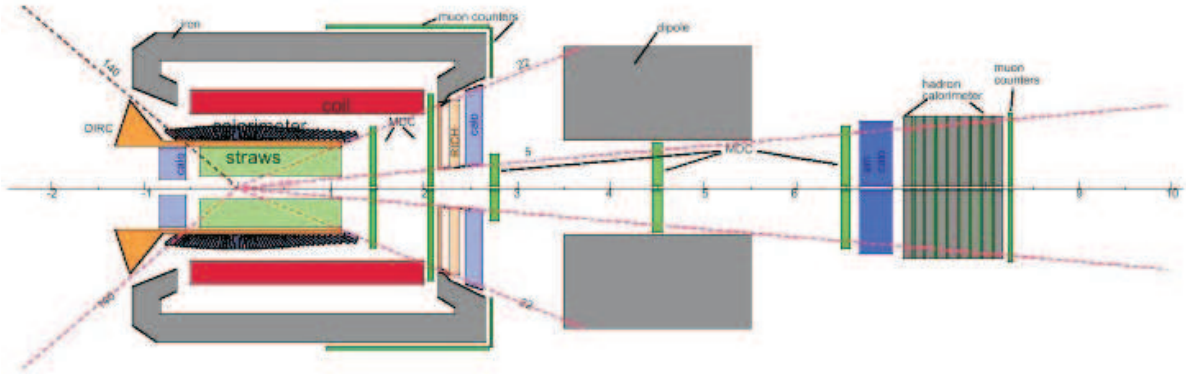


Fig. 9.4: Schematic view of the PANDA detector (side view)

diamond or silicon start detectors surrounding the interaction region followed by a 5-layer silicon microvertex detector; 15 layers of crossed straw tubes, for the measurement of charged-particle trajectories; a cylindrical DIRC and a forward aerogel Čerenkov detector for particle identification; an electromagnetic calorimeter consisting of $PbWO_4$ crystals with Avalanche Photo Diode (APD) readout. The region between the calorimeter and the end-cap will be instrumented with two sets of mini drift chambers; scintillator strips used for muon identification will be located behind the return yoke of the magnet.

The FS will measure particles emitted at polar angles below 10° in the horizontal and 5° in the vertical direction. It will consist of a dipole magnet with a 1 m gap, with MDCs before and after for charged-particle tracking. Particle identification will be achieved by means of a TOF stop and a dual-radiator RICH detector. Other components of the FS are an electromagnetic and a hadronic calorimeter followed by a set of muon chambers.

Detailed simulations of the detector concept presented here show its ability to measure electrons, muons, pions, kaons and photons over a large phase space region. Combining a momentum resolution of 1–2% with a high discriminating power for particle identification and a nearly $4\pi$ solid angle coverage allows the application of strong kinematical constraints, which will serve to achieve an excellent level of final-state identification and background suppression.

The PANDA project is part of the recently approved new accelerator facility at GSI. An international collaboration is currently forming to develop a detailed technical proposal for the design and construction of the detector system.

## 5.3 Physics programme

### *5.3.1 The ground state of charmonium, $\eta_c(1^1S_0)$*

Despite the abundance of experimental measurements, it is disappointing how little is known about the ground state of charmonium, $\eta_c(1^1S_0)$. Five new measurements of its mass were reported in 2002 and 2003, disagreeing by more than 5 MeV [15]. The fit to all existing measurements of the $\eta_c$ mass yields an error of 1 MeV (adequate to the accuracy of present theoretical model calculations), but the consistency between the various measurements is fairly poor (CL = 0.5%). In addition to that, as the accuracy of theoretical calculation increases it will be mandatory to measure its mass with a precision better than 1 MeV. The width of the $\eta_c$ is even more uncertain. Four new measurements were reported in 2002 and 2003, and the fit to all data yields a width value of $(25.0 \pm 3.3)$ MeV, with a CL of 0.05%. It is important to know the width of the $\eta_c$ because a width value as large as 25 MeV is difficult to reconcile with simple quark models, and it has been suggested that instanton effects may be responsible [16].

It must be stressed that unlike the E760/E835 experiments [17,18], which were obliged to identify $\eta_c$ formation in the extremely weak two-photon decay channel (BR$(\eta_c \to \gamma\gamma) \simeq 3 \times 10^{-4}$), the PANDA

detector at the new facility at GSI is being designed to detect both electromagnetic and hadronic final states. This will make it possible to study the $\eta_c$ in several decay channels, which have hundred times larger branching ratios: $\eta_c \to 2(K^+K^-), K\overline{K}\pi, 2(\pi^+\pi^-), \eta\pi\pi$, etc.

### *5.3.2 The radial excitation of charmonium, $\eta_c(2S)$*

The $\eta_c(2S)$ was discovered by the Belle experiment in the hadronic decays of the B meson [19], with a mass of $(3654 \pm 6 \pm 8)$ MeV, incompatible with the Crystall Ball observation [20]. The $\eta_c(2S)$ was then seen also by BaBar [21] and Cleo [22] in $\gamma\gamma$ collisions. The mass measurements of the three experiments are consistent [15] and yield a value of $(3637.7 \pm 4.4)$ MeV (CL = 14%); this value is only marginally consistent with most model calculations and it has been suggested that coupled channels effects may shift the $\eta_c(2S)$ mass [23]. The present accuracy on the $\eta_c(2S)$ width is only 50%, the measured value being $(19 \pm 10)$ MeV. More precise measurements of the mass and width are clearly needed.

A search for the $\eta_c(2S)$ was performed by the experiments E760 and E835 at Fermilab in the process $\overline{\mathrm{p}}\mathrm{p} \to \eta_c(2S) \to \gamma\gamma$ [17, 24]. No signal was observed by either experiment. The technique employed by E760/E835 suffered from the severe limitations due to the relatively high background from $\pi^0\pi^0$ and $\pi^0\gamma$ compared to the small $\gamma\gamma$ signal [25]. Further measurements using this channel will require increased statistics and a substantial reduction of the background. The real significant improvement of PANDA with respect to the Fermilab experiments will be the ability to detect the hadronic decay modes, such as $\eta_c(2S) \to K^*\overline{K}^*$ or $\eta_c(2S) \to \phi\phi$, which will allow a clean identification of this state.

### *5.3.3 The $h_c(^1P_1)$ resonance of charmonium*

The singlet P resonance of charmonium $h_c(^1P_1)$ is of extreme importance in determining the spin-dependent component of the $q\overline{q}$ confinement potential.

If the recent observation of $h_c$, described in Chapter 3, is confirmed during this decade, the precise measurement of its width will have to wait for the high statistics to be accumulated by the PANDA experiment. By comparing the total width with the probably dominant radiative width to $\eta_c\gamma$, it will be possible to measure its partial width to light hadrons, relevant for NRQCD calculations. It must be pointed out that owing to its very narrow width ($\leq 1$ MeV) and expected low yields, only a $\overline{\mathrm{p}}\mathrm{p}$ formation experiment like PANDA will be able to perform this measurement and to carry out a systematic study of its decay modes. The study of the $h_c$ constitutes a central part of the PANDA charmonium physics programme.

### *5.3.4 Radiative transitions of the $\chi_J(^3P_{0,1,2})$ charmonium states*

The measurement of the angular distributions in the radiative decay of the $\chi_1$ and $\chi_2$ states formed in $\overline{\mathrm{p}}\mathrm{p}$ annihilations provides insight into the dynamics of the formation process, the multipole structure of the radiative decay, and the properties of the $c\overline{c}$ bound state. A comparison of the E760 result at the $\chi_{c2}$ [26] with the Crystal Ball result at the $\chi_{c1}$ [27] is not consistent with theory, and may suggest the existence of additional contributions to the theoretical predictions for the M2 amplitudes. The simultaneous measurement of both angular distributions has been recently performed by E835 [28]. They too observed a discrepancy with respect to theoretical predictions, which could indicate the presence of competing mechanisms, leading to the cancellation of the M2 amplitude at the $\chi_{c1}$. The effect seen by E835 is at the $2.5\sigma$ level, therefore further high-statistics measurements are clearly needed to increase the significance of this result.

### *5.3.5 Charmonium states above the $\mathrm{D}\overline{\mathrm{D}}$ threshold*

The energy region above the $\mathrm{D}\overline{\mathrm{D}}$ threshold at 3.73 GeV will be object of many studies during this decade. This is the region in which narrow $^1\mathrm{D}_2$, $^3\mathrm{D}_2$ states (which are narrow because they cannot decay to $\mathrm{D}\overline{\mathrm{D}}$) and the first radial excitations of the singlet and triplet P states are expected to exist, as shown in Chapter 3. The discovery of X(3872) has raised further interest in this energy region: the nature of this

new, narrow state is not yet clear, and speculation ranges from a $\mathrm{D}^0\overline{\mathrm{D}^{0*}}$ molecule to a $^3\mathrm{D}_2$ state. There are theoretical problems with all these interpretations, and further, more accurate measurements of its width and particularly of its decay modes are needed to shed light on this state [23]. This kind of study is ideally suited for a $\overline{\mathrm{p}}\mathrm{p}$ formation experiment. The study of the energy region above the $\mathrm{D}\overline{\mathrm{D}}$ threshold is a central part of the charmonium physics programme of PANDA. It will require high-statistics, small-step scans of the entire energy region accessible at GSI.

### *5.3.6 Charmonium hybrids*

Predictions for hybrids come mainly from calculations based on the bag model, flux tube model, constituent gluon model and recently, with increasing precision, from lattice QCD (LQCD) [31]. For these calculations the parameters are fixed according to the properties of the known $Q\overline{Q}$ states. All model predictions and LQCD calculations agree that the masses of the lowest-lying charmonium hybrids are between 3.9 and 4.5 GeV and that the state with the lowest mass has $J^{PC} = 1^{-+}$ [32]. Some of the charmonium hybrids have spin exotic quantum numbers, so mixing effects with nearby $c\overline{c}$ states are excluded for them, thus making their experimental identification easier. Predictions for the widths of these states range from a few MeV to several tens of MeV. Cross-sections for the formation and production of charmonium hybrids are estimated to be similar to those of normal charmonium states.

In PANDA two kinds of experiments can be done: formation and production. Formation experiments would generate non-exotic charmonium hybrids, while production experiments would yield a charmonium hybrid together with another particle, such as a $\pi$ or an $\eta$. In $\overline{\mathrm{p}}\mathrm{p}$ annihilation, production experiments are the only way to obtain exotic quantum numbers. This distinction is a very powerful tool from the experimental point of view: the detection of a state in production and its non-detection in formation is a clear, unique signature for exotic behaviour.

### *5.3.7 Charmonium in nuclei*

The proposed experimental programme of PANDA will address open problems of in-medium modifications of hadrons with charmed quarks in nuclei and the interaction of these hadrons with nuclei. This is, on the one hand, an extension of the present chiral dynamics studies with partial restoration of chiral symmetry in the hadronic environment, from the light quark to the open charm quark sector. On the other hand, this programme is focused on the first experimental studies of the charmonium–nucleon and charmonium–nucleus interaction, which is also of basic importance for ultra-relativistic heavy-ion collisions.

## 6 JEFFERSON LAB 12 GEV UPGRADE

The Jefferson Laboratory has plans to upgrade the Continuous Electron Beam Accelerator Facility (CEBAF) to 12 GeV [33]. The 12 GeV electron beam will be used to produce 9 GeV photons in the new Hall D. Photon fluxes of up to $10^8$ photons/s with 50% linear polarization are achievable. In Hall D, a tagged coherent bremsstrahlung beam and solenoidal detector will be constructed in support of a programme of gluonic spectroscopy. The detector has been optimized to provide nearly hermetic acceptance for both charged particles and photons. In addition, a combination of particle identification systems will allow very good $K$–$\pi$ separation. Optimization will allow the detector to fully reconstruct exclusive many-body final states. In conjunction with high statistics, this will allow excellent partial wave analyses of many final states. The $4\pi$ acceptance of the Hall D detector and the energy resolution of its tagged beam could help to reduce the background considerably.

The threshold production of charmonium and open charm production open up a new window into QCD dynamics; in particular, these reactions are sensitive to multiquark, gluonic, and so-called 'hidden colour' correlations in nucleons and nuclei. In contrast to diffractive charm production at high energy, which tests the behaviour of the gluon structure functions at small $x$, charm production near threshold

tests the structure of the target near $x = 1$ and its short-range behaviour. This difference results from the kinematics of the reaction products. For $J/\psi$ production off the nucleon, the threshold energy is $E_\gamma = 8.2$ GeV and because of the large mass of the charmed quark the $c\bar{c}$ fluctuation of the photon travels over a short coherence length. Charm production near threshold implies a small impact parameter so that all five valence quarks must be in the same small interaction volume and all the quarks must be involved in the reaction mechanism. For nucleon targets this implies that three-gluon exchange may dominate two-gluon and one-gluon exchange.

Even though the $c\bar{c}$ pair is created with rather high momentum at threshold, it may be possible to observe reactions where the pair is captured by the target nucleus forming 'nuclear-bound quarkonium'. The discovery of such qualitatively new states of matter would be significant.

## 7 LHC (ATLAS/CMS)

The Large Hadron Collider (LHC) is a proton–proton collider currently being built at CERN and scheduled to start in the second half of 2007. It will provide many opportunities for studying heavy quarkonia, which will be produced at unprecedented rates and energies. Significant contributions may be expected in the fields of heavy quarkonia production and decays, whereas high background rates will make dedicated studies on heavy quarkonia spectroscopy difficult (as at other hadron machines).

This section concentrates on future opportunities at the two multipurpose LHC experiments ATLAS and CMS. Aspects related to the dedicated B-physics experiment LHCb and to studies 'in media' are covered in separate sections.

Heavy quarkonia production issues at the LHC in general are discussed in Section 7.1, and therefore apply to both ATLAS and CMS. Section 7.2 presents selected topics from current, heavy-quarkonia-related ATLAS studies. Results from CMS were not available at the time of writing. The selected topics are by no means comprehensive and are intended to serve as illustrative examples only.

### 7.1 Heavy quarkonia production at the LHC

Thanks to its high collision energy (design centre-of-mass energy 14 TeV) and high luminosity (design luminosity $\mathcal{L} = 10^{34}\ \mathrm{cm}^{-2}\mathrm{s}^{-1}$), the LHC will be able to explore a new high-energy frontier at the TeV scale. It is expected, however, that the LHC will not operate at its design luminosity from the beginning, but rather at an initial luminosity of $\mathcal{L} = 2 \times 10^{33}\ \mathrm{cm}^{-2}\mathrm{s}^{-1}$. This initial period will be best suited for dedicated studies on heavy quarkonia at the LHC, both in view of affordable trigger rates, modest pile-up (i.e., minimum-bias events superimposed on interesting signal), event reconstruction, etc.

The production rates for heavy quark flavours at the LHC will be huge. The total cross-section at the LHC is about 100 mb; the expected total cross-section for charm production is 7.8 mb, for bottom production 0.5 mb, and for top production 0.8 nb, respectively [34]. Thus, for an integrated luminosity of only 1 $\mathrm{fb}^{-1}$(i.e., about one week of running at initial luminosity), as many as $7.8 \times 10^{12}$ charm events, $0.5 \times 10^{12}$ bottom events, and $0.8 \times 10^{6}$ top events will be produced.

Figure 9.5 shows the differential cross-section for heavy-quark pair production at the LHC as a function of the transverse momentum of the heavy quark [34]. Up to next-to-leading-order (NLO) perturbative QCD, the $c$ and $b$ cross-sections are identical for high $p_\mathrm{T}$; differences due to mass effects show up only for very small $p_\mathrm{T}$ values ($p_\mathrm{T} < 20$ GeV). For orders higher than NLO, the spectrum for $c$ quarks is expected to become softer, and differences might become visible even for high $p_\mathrm{T}$.

In order to predict the production rates for heavy quarkonia at the LHC, the available models (including Monte Carlo generators) are tuned with Tevatron data and extrapolated to LHC energies; see [35] for a detailed description. Fig. 9.6 illustrates the results of this procedure applied to the prediction of the $J/\psi$ production cross-section. An eventual measurement of heavy quarkonia production rates at the LHC will help in understanding, for high energies and $p_\mathrm{T}$, the roles and importance of individual production mechanisms (e.g., colour-singlet vs. colour-octet) and the applicability of concepts used so

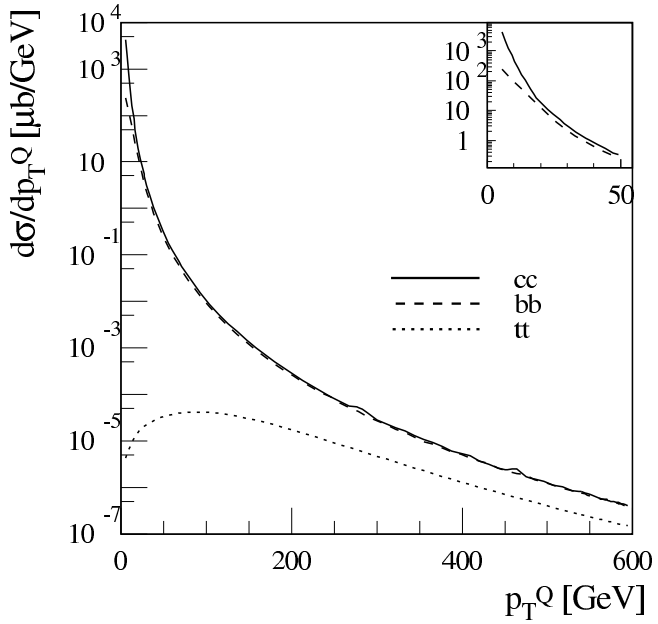


Fig. 9.5: Differential cross-section for heavy-quark-pair production as a function of the transverse momentum $p_{\mathrm{T}}^{Q}$ of the heavy quark. The smaller figure shows the region $p_{\mathrm{T}}^{Q} < 50$ GeV for charm and bottom production [34].

far in the calculations (e.g., factorisation in NRQCD). It might also be possible to probe the gluon density in the proton [36].

The fact that the LHC will produce heavy quarkonia with high transverse momentum in large numbers will also allow for a better discrimination between different models of heavy quarkonia polarization, like NRQCD and the colour-evaporation model; see Ref. [35]. For example, NRQCD predicts transversely polarized $J/\psi$ and $\psi(2S)$ (see Fig. 9.7) at high $p_{\mathrm{T}}$. This seems not to be supported by CDF data [42], although the statistics is too low to draw definitive conclusions. Measurements at the LHC will help in resolving the issue of quarkonium polarization.

## 7.2 Heavy quarkonia studies with ATLAS: selected topics

The ATLAS experiment has been designed both to maximize the discovery potential for new physics and to enable high-accuracy measurements. ATLAS also accommodates features which make it possible to incorporate an ambitious B-physics programme, in particular in the first years of running at low luminosity. Most of the foreseen studies on heavy quarkonia will be performed in the context of the B-physics programme. For a full review of the ATLAS detector and physics performance, see Ref. [34].

### *7.2.1 ATLAS B-Physics Trigger Issues*

ATLAS will have a flexible and efficient multi-level trigger system. The ATLAS trigger will consist of three levels, reducing the trigger rates from 40 MHz to $\mathcal{O}(20)$ kHz at level 1, to $\mathcal{O}(1$–$5)$ kHz at level 2, and to $\mathcal{O}(200)$ Hz at level 3 ('Event Filter', EF).

The classical B-physics trigger scenario [43] foresees to trigger for a muon with $p_{\mathrm{T}} > 6$ GeV and pseudo-rapidity $|\eta| < 2.4$ at level 1; to confirm this muon with better resolution and efficiency at level 2, together with performing a full scan of the Inner Detector (ID) to search for interesting signatures; and to refine the search at the EF level, where offline algorithms will be used and calibration and alignment data will be available.

In view of tight funding constraints, changes in detector geometry, the possible usage of a reduced detector at start-up, and a changed luminosity target at start-up ($1 \rightarrow 2 \times 10^{33}$ cm$^{-2}$s$^{-1}$), the classical

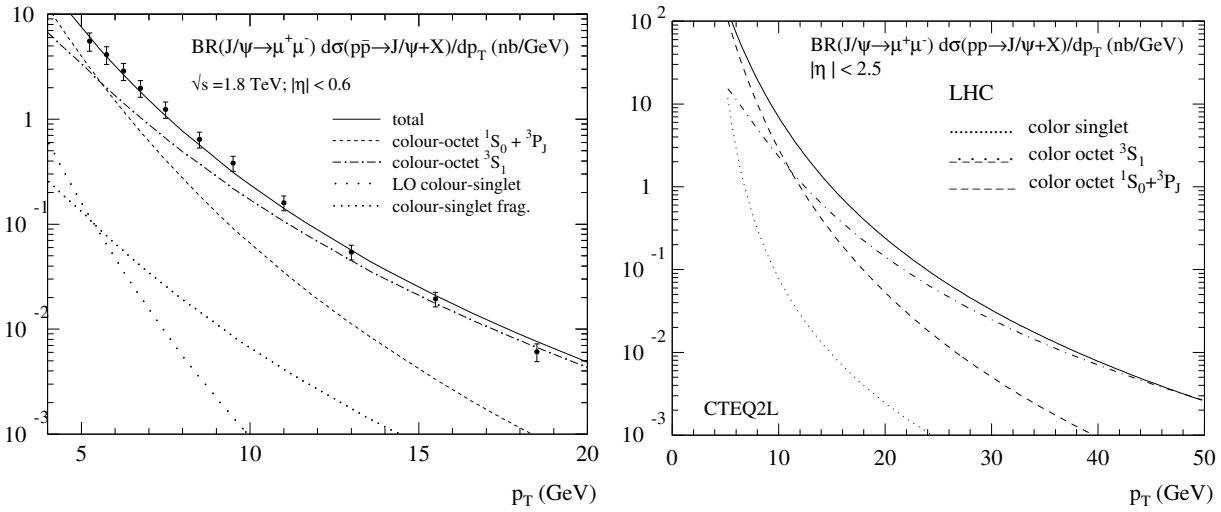


Fig. 9.6: Left: Colour-singlet and colour-octet contributions to direct $J/\psi$ production in $p\bar{p}\to J/\psi + X$ at the Tevatron, together with experimental data from CDF [38]. Right: cross-sections for $J/\psi$ production in $pp\to J/\psi + X$ at the LHC, as obtained with the Monte arlo generator PYTHIA supplemented by leading order colour-octet processes [39, 40]. Plots are taken from Refs. [35, 37].

scenario had to be revised; see Ref. [44] for details. In addition to more flexibility with respect to varying luminosity conditions, the revised scenario foresees additional trigger objects at level 1 (e.g., muon, 'Regions-of-Interest'/RoIs from calorimeter jet or electromagnetic triggers), and the RoI-guided search for tracks in the ID, in order to avoid the resource-intensive ID full scan. Studies are still ongoing, but first results look promising.

In the context of heavy quarkonia studies, the di-muon trigger will be the most important one. Fig. 9.8 shows the expected rates at a luminosity of $\mathcal{L} = 10^{33}$ cm$^{-2}$s$^{-1}$ [44]. The di-muon trigger will allow for an effective selection of channels with $J/\psi(\mu^+\mu^-)$, rare decays like B$\to\mu^+\mu^-$(X), etc. Minimum possible thresholds in the level 1 muon trigger are $p_{\rm T} > 5$ GeV (barrel) and $p_{\rm T} > 3$ GeV (end-cap), but the actual thresholds will be determined by the (yet incompletely known) level 1 muon rate. At higher trigger levels (level 2, EF), the muons from level 1 will be confirmed using the ID and Muon Detector precision chambers. Preliminary studies yield modest di-muon trigger rates of ∼200 Hz after level 2, and of ∼10 Hz after the EF, for the initial luminosity scenario of $\mathcal{L} = 2\times10^{33}$ cm$^{-2}$s$^{-1}$.

### *7.2.2 Recent ATLAS Studies on $J/\psi$*

The main emphasis in ongoing ATLAS physics-related studies lies on technical issues like validation and optimization of the architecture of trigger and offline software, performance, etc., not on doing full-fledged, detailed physics analyses. The results presented here are taken from a study on measuring the direct $J/\psi$ production cross-section, carried out in a wider context of studies on the performance of a staged (i.e., incomplete) detector in an initial commissioning period of 1 fb$^{-1}$ (corresponding to one year at 5% of the planned start-up luminosity).

The determination of the direct $J/\psi$ production cross-section will be one of the first B-physics measurements in ATLAS. There will be a large $J/\psi$ rate after the level 1 trigger, whose direct $J/\psi$ contribution will not be known. The measurement of the direct $J/\psi$ production cross-section is, among other things, important in order to find the best strategy for selecting $b$-events, e.g., to optimize the interplay between $p_{\rm T}$ and vertexing cuts.

Events of the type $pp\to J/\psi(\mu^+\mu^-)+X$ were generated with a version of PYTHIA which includes colour-octet processes [39–41]. One of the muons coming from $J/\psi$ was required to have $p_{\rm T} > 6$ GeV, the second to have $p_{\rm T} > 3$ GeV. For this purpose, functionality to enable filtering at generation time [45]

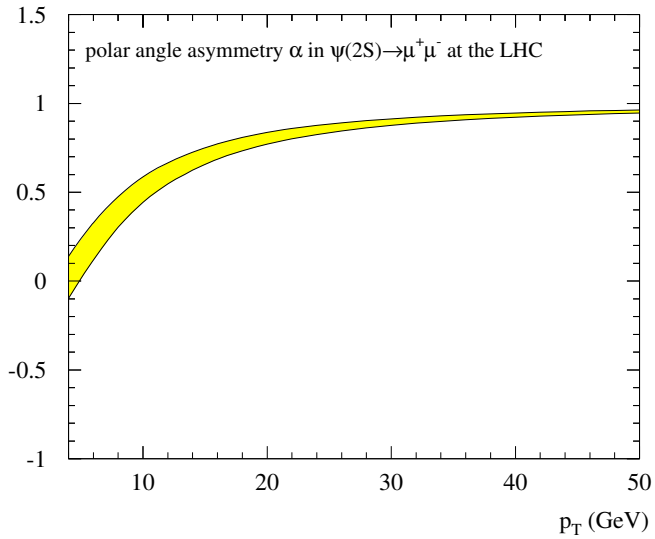


Fig. 9.7: Polar angle asymmetry $\alpha = (\sigma_T - 2\sigma_L)/(\sigma_T + 2\sigma_L)$ for $\psi(2S)$ production in $pp \to \psi(2S)(\to \mu^+\mu^-) + X$ at the LHC as a function of $p_{\rm T}$ [37].

was implemented into PYTHIA. Taking muons with $p_{\rm T}$ as low as 3 GeV is only possible when information from the hadronic calorimeter (Tile Calorimeter) is additionally taken into account, to allow for muon/hadron separation [34].

As a result, one obtains a cross-section for direct $J/\psi$ production of about 5 nb [45]. Typical values for relevant resolutions are primary vertex resolution $\sigma_{PV} < 15$ $\mu$m (given by the LHC beam cross-section); secondary vertex resolution $\sigma_{xy}(\text{core}) \simeq 70$ $\mu$m and $\sigma_{xy}(\text{tail}) \simeq 150$ $\mu$m; mass resolution $\sigma_{J/\psi} \simeq 40$ MeV. Preliminary studies suggest that, based on those performance parameters, a good separation of direct $J/\psi$'s and $J/\psi$'s from B-decays will be feasible. For a qualitative illustration, see Fig. 9.9.

### *7.2.3 Recent ATLAS Studies on $B_c$*

The expected large production rates at the LHC will also allow for precision measurements of $\mathrm{B_c}$ properties. Assuming a branching ratio $f(b \to \mathrm{B_c}) \simeq 10^{-3}$, an integrated luminosity of 20 fb$^{-1}$ (i.e., one year at initial luminosity), and requiring a level 1 muon with $p_{\rm T} > 6$ GeV and $|\eta| < 2.4$, recent estimates show that ATLAS will be able to record about 5600 events of the type $\mathrm{B_c} \to \mathrm{J}/\psi\,\pi$, and about 100 events of the type $\mathrm{B_c} \to \mathrm{B_s}\,\pi$.

The channels studied so far in ATLAS are $\mathrm{B_c} \to \mathrm{J}/\psi\,\pi$ for $\mathrm{B_c}$ mass measurement, and $\mathrm{B_c} \to \mathrm{J}/\psi\,\mu\nu$, since it provides a clean signature and can be used as an ingredient for determination of the CKM matrix element $|V_{cb}|$ [34]. Examples of older studies can be found in Ref. [46].

Since the production of $\mathrm{B_c}$ is suppressed by the hard production of an additional $c\bar{c}$ pair, Monte Carlo generation of $\mathrm{B_c}$ events using standard tools (e.g., PYTHIA) is CPU intensive. As an example, out of 100 000 PYTHIA pp events, one obtains about one $\mathrm{B_c}$ event, which in turn does not necessarily survive the ATLAS level 1 trigger selection. Recent developments in ATLAS have therefore concentrated on implementing dedicated $\mathrm{B_c}$ generators into PYTHIA. One approach is via the so-called 'Fragmentation Approximation Model', the other the so-called 'Full Matrix Element' (FME) approach [47].

The FME approach is based on the concept of extended helicity, i.e., the grouping of Feynman diagrams into gauge-invariant sub-groups to simplify the calculations, an approach never before followed in $gg \to QQ$ processes. It takes into account matrix elements from PQCD up to $\mathcal{O}(\alpha_s^4)$ (36 diagrams). Results obtained with the FME generator (subroutine BCVEGPY) in PYTHIA are shown in Figs. 9.10

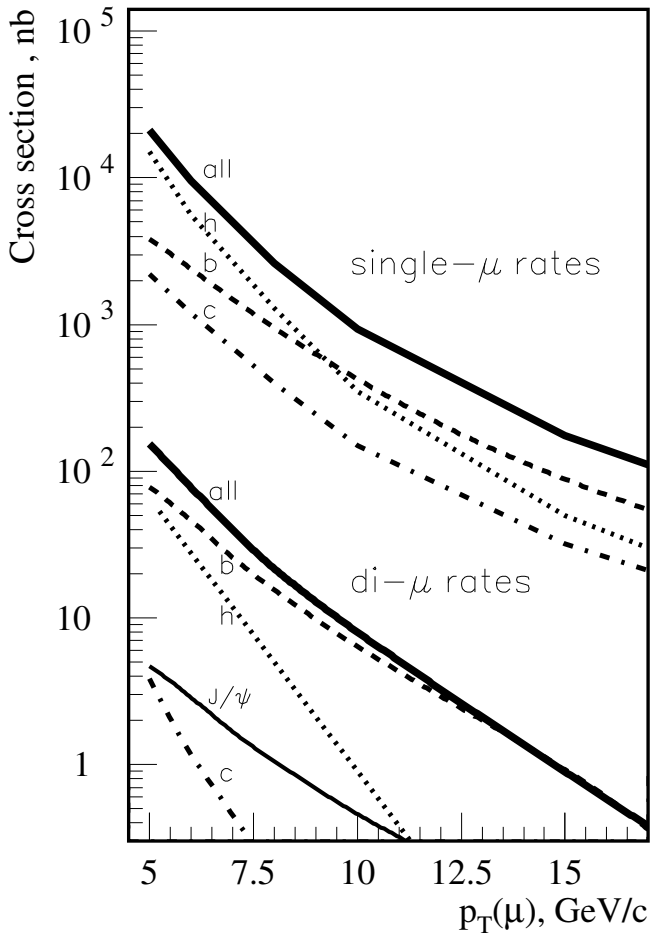


Fig. 9.8: Single-muon and di-muon cross-sections. Curves are shown for muons from $K$ and $\pi$ in-flight decays (labelled 'h'), $b$ and $c$ decays, and for the sum of all sources ('all'). Muons are considered within $|\eta| < 2.5$. For di-muons, the horizontal axis shows the $p_{\mathrm{T}}$ of the lower-$p_{\mathrm{T}}$ muon. At least one muon must have $p_{\mathrm{T}} > 6$ GeV and $|\eta| < 2.4$ according to level 1 trigger conditions [44].

(total cross-sections of $\mathrm{B_c}$ and $\mathrm{B_c^*}$ productions) and 9.11 ($\mathrm{B_c}$ pseudo-rapidity distribution). In terms of CPU performance, BCVEGPY is six times faster than other Monte Carlo generators available.

Studies on $\mathrm{B_c}$ physics performance in ATLAS are ongoing, where events generated by BCVEGPY /PYTHIA are passed through a full GEANT3 detector simulation and are subsequently reconstructed. As a preliminary result, a mass resolution of $\sigma_{B_c} = 74$ MeV was obtained in the channel $\mathrm{B_c} \rightarrow \mathrm{J}/\psi\,\pi$ for a staged-detector scenario.

### 7.3 Conclusions and outlook

The LHC will be a heavy quarkonia factory, producing them in high statistics up to large transverse momenta. Measurements of heavy quarkonia production rates at the LHC will be valuable for a deepened understanding of the production mechanisms involved and the applicability of the present theoretical approaches.

The multi-purpose experiments ATLAS (and CMS) at the LHC have the potential to play important roles in exploring the properties of heavy quarkonia. A deeper knowledge of heavy quarkonia properties is not only interesting as such, but also of vital interest for other physics fields, e.g., to understand the backgrounds occurring there.

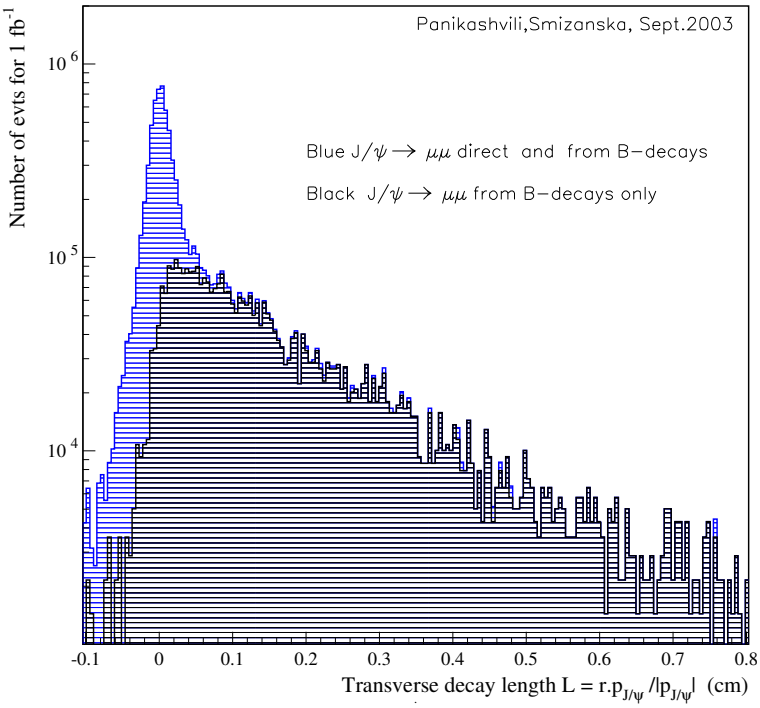


Fig. 9.9: The expected ATLAS potential for separating direct $J/\psi$'s and $J/\psi$'s from B-decays [45]. As discriminating variable, $L = \vec{r} \cdot \vec{p}_{J/\psi}/|\vec{p}_{J/\psi}|$ is used, where $\vec{r}$ and $\vec{p}_{J/\psi}$ denote the vectors of transverse $J/\psi$ decay radius and transverse $J/\psi$ momentum, respectively.

ATLAS is planning to continue the studies on heavy quarkonia in the future, including topics not covered until now like cross-section measurements for $\psi(2S)$ or for the process $\chi_c \to J/\psi\,\gamma$, polarization measurements, and studies on $\Upsilon$ states.

## 8 LHCb

### 8.1 The LHCb detector

The LHCb detector is designed to exploit the large number of b-hadrons produced at the LHC in order to make precision studies of CP asymmetries and of rare decays in the B-meson systems. It has a high-performance trigger which is robust and optimized to collect B mesons efficiently, based on particles with large transverse momentum and displaced decay vertices.

The detector can reconstruct a B-decay vertex with very good resolution and provide excellent particle identification for charged particles. Excellent vertex resolution is essential for studying the rapidly oscillating $\mathrm{B_s}$ mesons and in particular their CP asymmetries. It also helps to reduce combinatoric background when reconstructing rare decays.

The LHCb experiment plans to operate with an average luminosity of $2 \times 10^{32}\ \mathrm{cm^{-2}\ s^{-1}}$, which should be obtained from the beginning of the LHC operation. Running at this luminosity has further advantages. The detector occupancy remains low, and radiation damage is reduced. Events are dominated by single pp interactions that are easy to analyse. The luminosity at the LHCb interaction point can be kept at its nominal value while the luminosities at the other interaction points are being progressively increased to their design values. This will allow the experiment to collect data for many years under constant conditions. About $10^{12}\ \mathrm{b\overline{b}}$ pairs are expected to be produced in one year of data taking.

In addition to investigating CP violation in B-meson decays, the physics programme of the LHCb experiment will include studies of rare B and $\tau$ decays, D–$\overline{\mathrm{D}}$ oscillations and $\mathrm{B_c}$-meson decays.

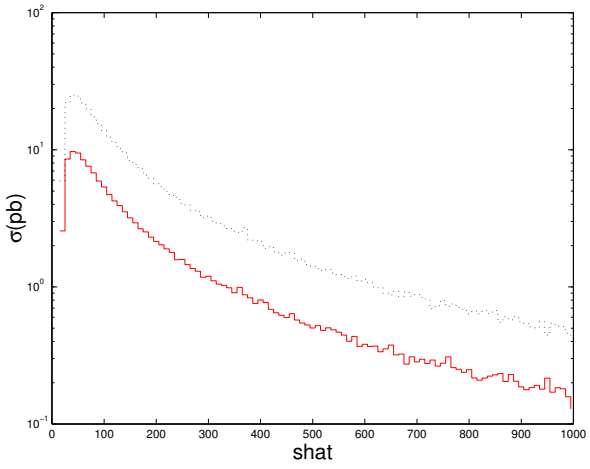


Fig. 9.10: Integrated cross-sections for the sub-process $gg \to \mathrm{B_c}(\mathrm{B_c^*}) + \mathrm{b} + \bar{\mathrm{c}}$ as obtained with the BCVEGPY Monte Carlo generator [47]. The solid (dotted) line corresponds to $\mathrm{B_c}$ ($\mathrm{B_c^*}$) production. 'shat' denotes $\sqrt{s}$, the centre-of-mass energy of the sub-process.

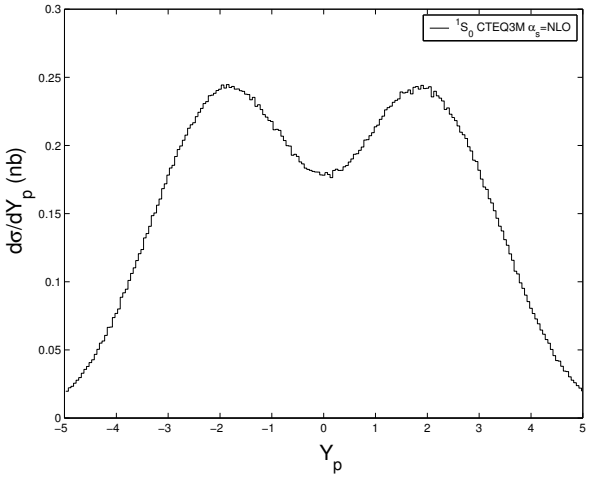


Fig. 9.11: The $\mathrm{B_c}$ pseudo-rapidity distribution obtained with the parton distribution function CTEQ3M. For details see Ref. [47].

Fig. 9.12 shows the layout of the LHCb detector. It consists of the beam pipe, VELO (VErtex LOcator), dipole magnet, tracking system, two Ring Imaging Cherenkov detectors with three radiators (RICH1 and RICH2), calorimeter system and muon system.

The trigger system is designed to suppress the initial rate of about 40 MHz to approximately 200 Hz by selecting the events with high-$p_{\mathrm{T}}$ hadrons, leptons and photons, requiring secondary vertices, and performing partial event online reconstruction to select the desired b-hadron decays. The trigger system is designed to be flexible, robust and efficient. Events are selected by various criteria that can be easily adjusted according to the experimental conditions. For a full review of the LHCb detector and physics performance, see Refs. [48, 49].

### 8.2 Recent LHCb studies on $\mathrm{B_c}$

The $\mathrm{B_c}$ meson is the ground state of the $\bar{b}c$ system which in many respects is an intermediate between charmonium and bottomonium systems. However, since the $\mathrm{B_c}$ mesons carry flavour, they provide a window for studying heavy-quark dynamics very different from that of by $c\bar{c}$- and $b\bar{b}$-quarkonia.

The $\bar{b}c$ system exhibits a rich spectroscopy of orbital and angular-momentum excitations, radiative and weak decays. In addition, the $\mathrm{B_c}$ also provides a good place for extracting the Cabibbo–Kobayashi–Maskawa (CKM) matrix elements $V_{cb}$ and $V_{ub}$. Two-body hadronic decays of $\mathrm{B_c}$ mesons can play an important role for the exploration of CP violation. For a recent review of the $\mathrm{B_c}$ physics issues, see Ref. [50].

The production of $\mathrm{B_c}$ states at high $p_{\mathrm{T}}$ is well described by b-quark fragmentation, while the complete $O(\alpha_s^4)$ calculations show the dominance of the recombination mechanism in the low-$p_{\mathrm{T}}$ region (see Fig. 9.13 where the $p_{\mathrm{T}}$ dependence of $\mathrm{B_c}$ and $\mathrm{B_c^*}$ production is shown).

The low-$p_{\mathrm{T}}$ region is dominated by high-momentum $\mathrm{B_c}$ (see Fig. 9.14) that gives additional advantages for the LHCb detector where $\mathrm{B_c}$ meson decays will produce secondary vertices well separated from the primary one. This fact ensures that $\mathrm{B_c}$ decays will satisfy the LHCb trigger conditions and provides the possibility of strong background suppression.

The exclusive decay channel $\mathrm{B_c^\pm} \to \mathrm{J}/\psi\pi^\pm$, $\mathrm{J}/\psi \to \mu^+\mu^-$ has been studied in Ref. [51]. $\mathrm{B_c}$ mesons with $m = 6.4$ GeV and $\tau = 0.47$ ps were used for the signal Monte Carlo. The main background

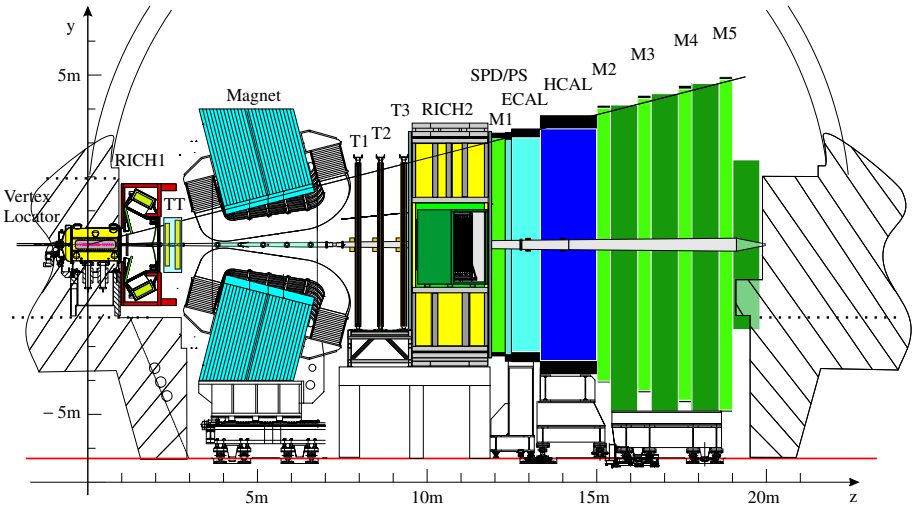


Fig. 9.12: LHCb detector layout

comes from the prompt $J/\psi$ production ($\sim 0.8$ mb) and $\mathrm{B}\to\mathrm{J}/\psi\mathrm{X}$ decays. The complete GEANT simulation of the signal and background events (including minimum-bias background) has been performed with the detailed description of the detector response. Trigger algorithms have been applied, $\mathrm{B_c}\to\mathrm{J}/\psi\pi$ candidates have been reconstructed using full pattern recognition, and specific offline cuts have been applied to reject background.

The mass resolution is shown in Fig. 9.15 with the shaded area representing the surviving background. A clean and narrow signal is observable, with an expectation of about 14 k $\mathrm{B_c}\to\mathrm{J}/\psi\pi$ decays reconstructed per year with a $B/S$ ratio estimated to be $< 0.8$.

The reconstructed events were used to determine the $\mathrm{B_c}$ lifetime as well. The difference between true and reconstructed lifetime is shown in Fig. 9.16. The proper time resolution is about 0.04 ps and can be improved using high-momentum $\mathrm{B_c}$ mesons.

LHCb is planning to study $\mathrm{B_c}$ mesons production including radiative $\mathrm{B_c^*}$ decays as well as other ground-state decay channels.

## 9 ALICE

ALICE is the dedicated heavy-ion experiment at the LHC. The apparatus will investigate the properties of strongly interacting matter at extreme energy density where the formation of quark–gluon plasma (QGP) is expected [52]. For this purpose, heavy quarkonium states are especially relevant since they provide, via their leptonic decays, an essential probe of the medium produced in the collision. A lot of effort has been devoted to the subject (for reviews see Refs. [53, 54]) since the early predictions of charmonium suppression by Debye screening in a deconfined medium [55]. The LHC energy is unique for such studies since it allows, for the first time, the spectroscopy of charmonium and bottomonium resonances in heavy-ion collisions. In particular, because the $\Upsilon(1S)$ is expected to dissolve only significantly above the critical temperature [56,57], the spectroscopy of the $\Upsilon$ family at LHC energies should reveal unique information on the characteristics of the QGP [58]. On the other hand, the study of heavy-quark resonances in heavy-ion collisions at the LHC is subject to significant differences with respect to lower energies. First, in addition to prompt charmonia produced directly via hard scattering, secondary charmonia can be produced from bottom decay [59], $\mathrm{D\bar{D}}$ annihilation [60], and by coalescence mechanisms which could result in enhancement rather than suppression [61]. Then, in the environment of a heavy-ion reaction, in-medium effects such as shadowing and heavy-quark energy loss may substantially modify the final yields and spectra [61]. Open charm and open beauty production is another important issue addressed

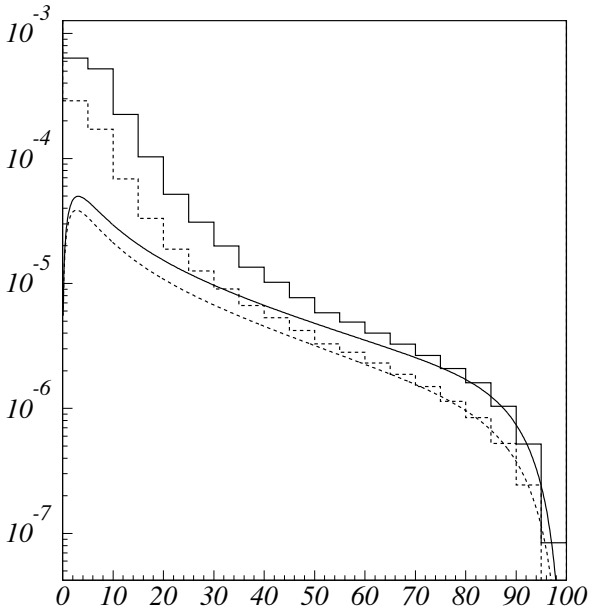


Fig. 9.13: $O(\alpha_s^4)$ calculations (histograms) and fragmentation model (curves) for vector (solid) and pseudo-scalar (dashed) $\mathrm{B_c}$ mesons production at $\hat{s} = 200$ GeV. The horizontal axis denotes the $\mathrm{B_c}$ transverse momentum.

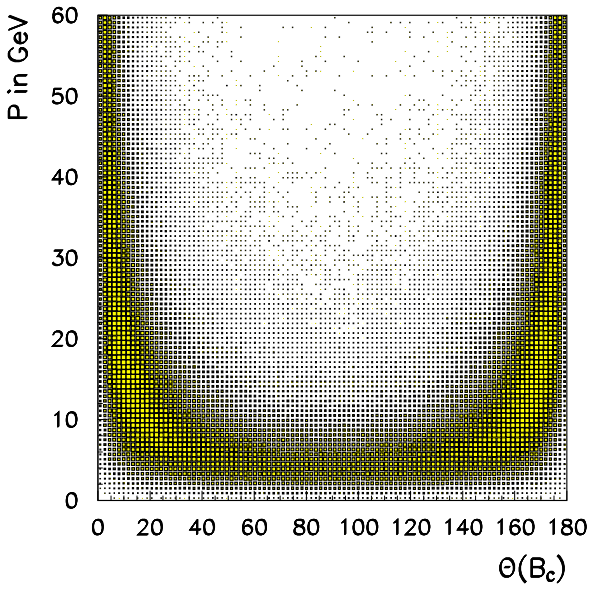


Fig. 9.14: The momentum $P(\mathrm{B_c})$ vs. the angle between the momentum of the $\mathrm{B_c}$ and the $z$-axis in the laboratory system at LHC energies.

by ALICE since they provide the most natural normalization to quarkonia suppression/enhancement. On the other hand, in a QGP, an additional source of charm quarks may arise from secondary parton scattering [62, 63] and information on the properties of the deconfined medium could be revealed by the kinematical properties of heavy mesons.

ALICE will allow measurements of heavy flavours in both the muon and the electron channels as well as full reconstruction of D mesons in the hadronic channel. Although the apparatus is dedicated to heavy-ion collisions, proton–proton and proton–nucleus collisions are also an important part of the ALICE physics programme in order to unravel initial and final-state medium effects.

## 9.1 ALICE detector

The ALICE detector [64] is designed to cope with large particle multiplicities which, in central Pb–Pb collisions, are expected to be between 2000 and 8000 per unit rapidity at mid rapidity. It consists of a central part, a forward muon spectrometer, and forward/backward small acceptance detectors. The central part of ALICE consists of four layers of detectors placed in the solenoidal field ($B < 0.5$ T) provided by the LEP L3 magnet. From the inner side to the outer side, these detectors are the Inner Tracker System (ITS), the large Time Projection Chamber (TPC), the Transition Radiation Detector (TRD) and the Time of Flight system (TOF). They provide charged-particle reconstruction and identification in the pseudo-rapidity range $|\eta| < 0.9$, with full azimuthal coverage and a broad $p_{\mathrm{T}}$ acceptance. These large-area devices are complemented by smaller acceptance detectors: the High-Momentum Particle Identification (HMPID), the PHOton Spectrometer (PHOS) and the Photon Multiplicity Detector (PMD). In the forward/backward region, the charged multiplicity and the zero degree energy will be measured by additional detectors (T0, V0, FMD, ZDC) which will allow fast characterization and selection of the events. Finally, a forward muon spectrometer covering the pseudo rapidity range $2.5 < \eta < 4$ is placed on the right side of the central part. It consists of a front absorber, a dipole magnet, ten high-granularity tracking chambers, a muon filter, and four large-area trigger chambers.

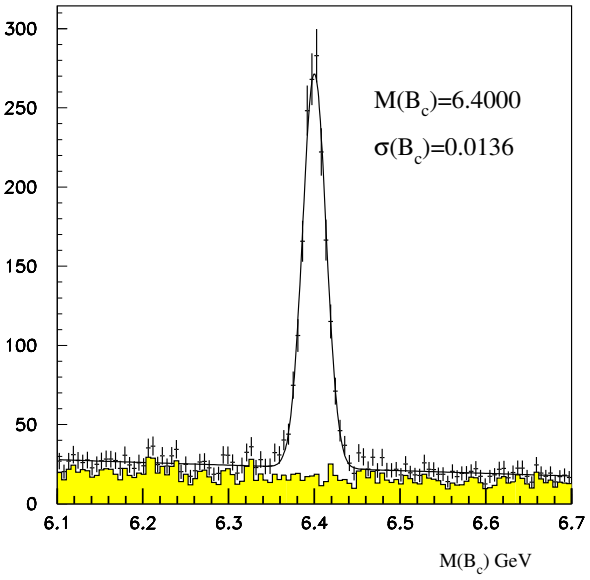


Fig. 9.15: The reconstructed $B_c$ mass with background. The curve is a Gaussian plus polynomial fit.

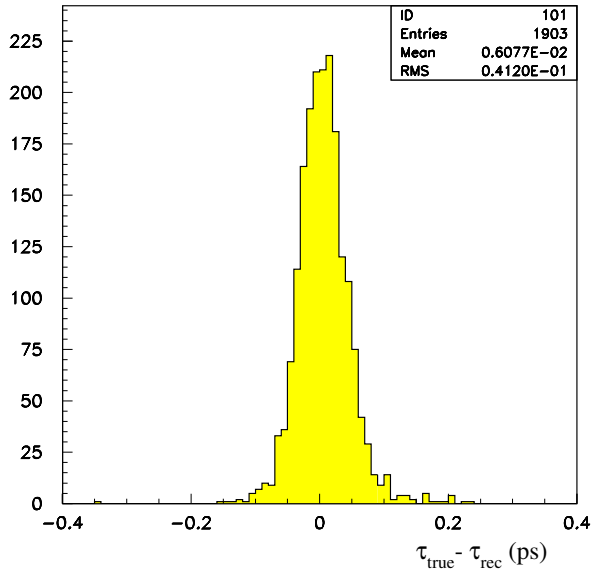


Fig. 9.16: Comparison of the reconstructed and generated $B_c$ lifetime

## 9.2 Muons

The goal of the forward muon spectrometer [65] is to measure the full set of onium resonances from the $\phi$ to the $\Upsilon$, with high statistics, a low background, and a high resolution. The spectrometer is equipped with a dimuon trigger based on the selection of pairs of muons with large transverse momentum. An important specification of the spectrometer is its mass resolution which has to be about 100 MeV at 10 GeV to allow the separation of the $\Upsilon$ substates. Detailed simulations have shown that this goal should be reached, even in the worst scenario of background environment that could be foreseen. The acceptance for $J/\psi$ and $\Upsilon$ is fairly uniform in $p_{\mathrm{T}}$ and allows both $J/\psi$ and $\Upsilon$ to be detected down to $p_{\mathrm{T}} = 0$. The statistics expected in a $10^6$ s run, roughly corresponding to one month of data taking, is of $\sim 500 \times 10^3$ $J/\psi$ and $\sim 10000$ $\Upsilon$ in minimum-bias Pb–Pb collisions. For $J/\psi$, the rate and signal-over-background (S/B) are very good and permit a high-precision measurement of the differential cross-section. The $\psi(2S)$ can be measured at best with an accuracy of the order of 10% because of less favourable S/B. For the $\Upsilon$ family, the S/B is larger than unity and the significance is 70, 31 and 22 for $\Upsilon(1S)$, $\Upsilon(2S)$ and $\Upsilon(3S)$. In addition to quarkonia measurements, the spectrometer will allow measurements of the differential open bottom cross-section. This will be achieved both in the single muon and the dimuon channels.

## 9.3 Electrons

The measurement of dielectrons in the central barrel of ALICE is complementary to the dimuon channel. It extends quarkonia measurements from the forward rapidity region to mid-rapidity and allows one to measure secondary $J/\psi$ from bottom decay thanks to the vertex capabilities of the ITS. This will permit the distinction between primary and secondary $J/\psi$ and also lead to a direct measurement of the B-meson production cross-section. Furthermore, single high-$p_{\mathrm{T}}$ electrons with displaced vertex give access to the inclusive open charm and open bottom cross-sections. The centrepiece for dielectron physics is the TRD which provides an electron trigger and identification [66]. Its acceptance is identical to that of the ITS/TPC ($|\eta| < 0.9$ with full azimuthal coverage). Its expected pion rejection factor in a high-multiplicity environment has been investigated by means of detailed simulations. These simulations were adjusted to test beam data for well isolated tracks and then performed for various track multiplicities. Going from well isolated tracks to a full multiplicity event (8000 charged particles per unit of rapidity at mid-rapidity), a worsening of the pion rejection by a factor 6–7 is observed. For an electron efficiency

of 90% the pion rejection factor is still better than 50. On the other hand, the track reconstruction using information from the ITS, TPC and TRD leads to a $\Upsilon$ mass resolution good enough for the separation of the $\Upsilon$ substates.

### 9.4 Hadrons

In the central part of ALICE, heavy mesons can be fully reconstructed from their charged-particle decay products in the ITS, TPC and TOF. Thus, not only their integrated yields, but also their $p_{\rm T}$ distributions can be measured. The most promising decay channel for open charm detection is the $\rm D^0 \to K^- \pi^+$ decay (and its charge conjugate) which has a branching ratio of about 3.8% and $c\tau = 124\ \mu$m. The expected rates (per unit of rapidity at mid rapidity) for $\rm D^0$ (and $\rm \bar{D}^0$) mesons, decaying in a $K^\mp \pi^\pm$ pair, in central (5%) Pb–Pb at $\sqrt{s} = 5.5$ TeV and in pp collisions at $\sqrt{s} = 14$ TeV are $5.3 \times 10^{-1}$ and $7.5 \times 10^{-4}$ per event, respectively. The selection of this decay channel allows the direct identification of the $\rm D^0$ particles by computing the invariant mass of fully-reconstructed topologies originating from displaced secondary vertices. The expected statistics are $\simeq$ 13 000 reconstructed $\rm D^0$ in $10^7$ central Pb–Pb events and $\simeq$ 20 000 in $10^9$ pp events. The significance is larger than 10 for up to about $p_{\rm T} = 10$ GeV both in Pb–Pb and in pp. The cross-section can be measured down to $p_{\rm T} \simeq 1$ GeV in Pb–Pb collisions and down to almost $p_{\rm T} = 0$ in pp collisions.

### REFERENCES


[1] P. Mathews, P. Poulose and K. Sridhar, Phys. Lett. B **438**, 336 (1998) [arXiv:hep-ph/9803424].

[2] K. Sridhar, Phys. Rev. Lett. **77**, 4880 (1996) [arXiv:hep-ph/9609285].

[3] C. Qiao, F. Yuan and K. Chao, Phys. Rev. D **55**, 5437 (1997) [arXiv:hep-ph/9701249].

[4] C. S. Kim, J. Lee and H. S. Song, Phys. Rev. D **55**, 5429 (1997) [arXiv:hep-ph/9610294].

[5] P. Mathews, K. Sridhar and R. Basu, Phys. Rev. D **60**, 014009 (1999) [arXiv:hep-ph/9901276].

[6] V. Barger, S. Fleming and R. J. Phillips, Phys. Lett. B **371**, 111 (1996) [arXiv:hep-ph/9510457].

[7] E. Braaten, S. Fleming, and A. K. Leibovich, Phys. Rev. D **63**, 094006 (2001) [arXiv:hep-ph/0008091].

[8] F. Maltoni and A. D. Polosa, Phys. Rev. D **70**, 054014 (2004) [arXiv:hep-ph/0405082].

[9] E. Braaten, J. Lee and S. Fleming, Phys. Rev. D **60**, 091501 (1999) [arXiv:hep-ph/9812505].

[10] R. A. Briere *et al.*, CLNS-01-1742.

[11] S. K. Choi *et al.* [BELLE collaboration], Phys. Rev. Lett. **89**, 102001 (2002) [Erratum-ibid. **89**, 129901 (2002)] [arXiv:hep-ex/0206002].

[12] D. M. Asner *et al.* [CLEO Collaboration], Phys. Rev. Lett. **92**, 142001 (2004) [arXiv:hep-ex/0312058].

[13] F. E. Close, G. R. Farrar and Z. p. Li, Phys. Rev. D **55**, 5749 (1997) [arXiv:hep-ph/9610280].

[14] *An International Accelerator Facility for Beams of Ions and Antiprotons*; Conceptual Design Report, November 2001. http://www.gsi.de/GSI-Future/cdr .

[15] T. Swkarnicki, *Heavy Quarkonia*, Proceedings of XXI International Symposium on Lepton and Photon Interactions at High Energies, Fermilab, August 2003, To be published.

[16] M. B. Voloshin, private communication.

[17] E760 Collaboration, T.A. Armstrong *et al.*, Phys. Rev. D **52**, 4839 (1995).

[18] E835 Collaboration, M. Ambrogiani *et al.*, Phys. Lett. B **566**, 45 (2003).

[19] Belle Collaboration, S.K. Choi *et al.*, Phys. Rev. Lett. **89**, 102001 (2002);
Belle Collaboration, K. Abe *et al.*, Phys. Rev. Lett. **89**, 142001 (2002).

[20] Crystal Ball Collaboration, C. Edwards *et al.*, Phys. Rev. Lett. **48**, 70 (1982).

[21] B. Aubert *et al.* [BABAR Collaboration], Phys. Rev. Lett. **92**, 142002 (2004) [arXiv:hep-ex/0311038].

[22] CLEO Collaboration, T. Ferguson, *Observation of $\eta_c$ in two-photon collisions at CLEO*, presentation given at the Second QWG Workshop on Heavy Quarkonia, http://www.qwg.to.infn.it/WS-sep03/WS2talks/spectr/ferguson.pdf .

[23] S. Godfrey, *Quarkonium spectroscopy*, presentation given at the Second QWG Workshop on Heavy Quarkonia, http://www.qwg.to.infn.it/WS-sep03/WS2talks/spectr/godfrey_pot.pdf.

[24] E835 Collaboration, M. Ambrogiani *et al.*, Phys. Rev. D **64**, 052003 (2001).

[25] E760 Collaboration, T.A. Armstrong *et al.*, Phys. Rev. D **56**, 2509 (1997).

[26] E760 Collaboration, T.A. Armstrong *et al.*, Phys. Rev. D **48**, 3037 (1993).

[27] Crystal Ball Collaboration, M. Oreglia *et al.*, Phys. Rev. D **25**, 2259 (1982).

[28] E835 Collaboration, M. Ambrogiani *et al.*, Phys. Rev. D **65**, 052002 (2002).

[29] Belle Collaboration, S.K. Choi *et al.*, Phys. Rev. Lett. **91**, 262001 (2003) [arXiv:hep-ex/0309032].

[30] CDF Collaboration, G. Bauer, *Observation of a Narrow State Decaying to $J/\psi\pi^+\pi^-$ in CDF*, presentation given at the Second QWG Workshop on Heavy Quarkonia, http://www.qwg.to.infn.it/WS-sep03/WS2talks/spectr/plenary/bauer.ps.gz.

[31] P. Chen, X. Liao and T. Manke, Nucl. Phys. Proc. Suppl. **94**, 342 (2001); C. Michael, Proceedings of Heavy Flavours 8, Southampton, UK, 1999.

[32] T. Barnes, F.E. Close and E.S. Swanson, Phys. Rev. D **52**, 5242 (1995).

[33] The Science Driving the 12 GeV Upgrade of CEBAF, Jefferson Lab, 2001.

[34] ATLAS Collaboration, *ATLAS Detector and Physics Performance Technical Design Report Vol. I*, CERN/LHCC/99-14; *Vol. II*, CERN/LHCC/99-15 (May 1999).

[35] P. Nason *et al.*, hep-ph/0003142 (2000); published in M. Mangano, G. Altarelli (ed.), *1999 CERN Workshop on Standard Model Physics (and More) at the LHC*, CERN-2000-004 (2000).

[36] J. L. Domenech-Garret, M. A. Sanchis-Lozano and S. Wolf, J. Phys. G **28**, 687 (2002) [arXiv:hep-ph/0110085].

[37] M. Krämer, Prog. Part. Nucl. Phys. **47**, 141 (2001) [arXiv:hep-ph/0106120].

[38] F. Abe *et al.*, CDF Collaboration, Phys. Rev. Lett. **79**, 572 (1997).

[39] M. A. Sanchis-Lozano, Nucl. Phys. Proc. Suppl. **86**, 543 (2000) [arXiv:hep-ph/9907497].

[40] M. A. Sanchis-Lozano, Nucl. Phys. Proc. Suppl. B **75**, 191 (1999) [arXiv:hep-ph/9810547].

[41] B. Cano-Coloma and M. A. Sanchis-Lozano, Nucl. Phys. B **508**, 753 (1997) [arXiv:hep-ph/9706270].

[42] T. Affolder *et al.*, CDF Collaboration, Phys. Rev. Lett. **85**, 2886 (2000).

[43] ATLAS Collaboration, *ATLAS High-Level Triggers, DAQ and DCS Technical Proposal*, CERN/LHCC/2000-017 (March 2000).

[44] ATLAS Collaboration, *ATLAS High-Level Trigger, Data Acquisition and Controls Technical Design Report*, CERN/LHCC/2003-022 (June 2003).

[45] N. Panikashvili, private communication; write-up as ATLAS Internal Note ATL-COM-PHYS-2003-048 (2003).

[46] F. Albiol, R. Pérez Ochoa, M. A. Sanchis-Lozano and J. A. Valls, hep-ph/9506306 (1995); M. Galdón, R. Pérez Ochoa, M. A. Sanchis-Lozano and J. A. Valls, hep-ph/9510450 (1995).

[47] C. H. Chang, C. Driouichi, P. Eerola and X. G. Wu, Comput. Phys. Commun. **159**, 192 (2004) [arXiv:hep-ph/0309120].

[48] LHCb Collaboration, S. Amato *et al*, Technical Proposal, CERN-LHCC/98-4.

[49] LHCb Collaboration, R. Antunes Nobrega *et al*, Technical Design Report. Reoptimized Detector Design and Performance, CERN/LHCC 2003-030.

[50] I.P. Gouz, V.V. Kiselev, A.K. Likhoded, V.I. Romanovski and O.P. Yushchenko, Phys. Atom. Nucl. **67**, 1559 (2004) and hep-ph/0211432 (2002).

[51] O.P. Yushchenko, Search for the $B_c^+ \to J/\psi(\mu^+\mu-)\pi^+$ decay with the LHCb spectrometer, LHCb-note 2003-113.

[52] ALICE Collaboration, ALICE Physics Performance Report, in preparation; ALICE Collaboration internal note, ALICE-INT-2002-25.

[53] H. Satz, Rep. Prog. Phys. **63**, 1511 (2000) [arXiv:hep-ph/0007069].

[54] R. Vogt, Phys. Rep. **310**, 197 (1999) .

[55] T. Matsui and H. Satz, Phys. Lett. B **178**, 416 (1986).

[56] S. Digal, P. Petreczky and H. Satz, Phys. Rev. D **64**, 094015 (2001) [arXiv:hep-ph/0106017].

[57] C. Y. Wong, Phys. Rev. C **65**, 034902 (2002) [nucl-th/0110004].

[58] J. F. Gunion and R. Vogt, Nucl. Phys. B **492**, 301 (1997) [arXiv:hep-ph/9610420].

[59] S. Eidelman *et al.* [Particle Data Group Collaboration], Phys. Lett. B **592**, 1 (2004).

[60] P. Braun-Munzinger and K. Redlich, Eur. Phys. J. C **16**, 519 (2000) [arXiv:hep-ph/0001008].

[61] M. Bedjidian *et al.*, Workshop on Hard Probes in Heavy–Ion Collisions at the LHC, CERN–2004–009, [arXiv:hep-ph/0311048].

[62] B. Müller and X.N. Wang, Phys. Rev. Lett. **68**, 2437 (1992).

[63] K. Geiger, Phys. Rev. D **48**, 4129 (1993).

[64] http://alice.web.cern.ch/Alice/AliceNew/ .

[65] ALICE Collaboration, TDR of the muon Spectrometer, CERN/LHCC 99-22 (1999); Addendum 1 to the TDR of the muon Spectrometer, CERN/LHCC 2000-046 (2000).

[66] ALICE Collaboration, TDR of the TRD, CERN/LHCC 2001-021 (2001).